Optical Properties of Zinc Oxide Nanoparticles Prepared by a One-Step Mechanochemical Synthesis Method

Zahra Makhdoumi Kakhaki,[*] Amirali Youzbashi and Nima Naderi

Materials and Energy Research Center, P.O. Box 14155-4777, Tehran, Iran

[*]Corresponding author: zahramakhdoomi@yahoo.com

Abstract: *ZnO nanoparticles were synthesised by a one-step mechanochemical process using ZnSO₄ and NaOH as reactants with NaCl acting as a diluent. A short milling time of 30 min was required for complete reaction. The effects of oxygen vacancies and the milling time on the photocatalytic activities of the prepared nanoparticles were investigated. The structural and morphological properties of the nanoparticles were evaluated by various analytical methods, including x-ray diffraction, scanning electron microscopy, and transmission electron microscopy. The particle size of the ZnO nanoparticles without heat treatment was approximately 50 nm but was increased up to 80 nm after heat treatment at 400°C. Optical properties such as the optical band gap and the photocatalytic activity were investigated by photoluminescence and UV-vis spectroscopy, as well as by photocatalytic experiments.*

1.   INTRODUCTION

ZnO nanoparticles have found widespread application in a range of industries, including use as solar cells,[1] photocatalysts,[2] gas sensors,[3] optoelectronic devices[4] and photonic devices,[5] due to their exceptional properties. These properties include their wide band gap in the bulk state (3.37 ev) and large exciton energy (60 meV) at room temperature.[6] Various methods have been reported for the syntheses of ZnO nanoparticles, including precipitation,[7,8] spray pyrolysis,[9] hydrothermal,[10] sol-gel,[11] thermal evaporation,[12] mechanical[13] and mechanochemical[14–19] methods. The mechanochemical method is one of the most frequently utilised methods for the synthesis of ZnO nanoparticles because of its notable advantages, such as its adaptability to large-scale production, low cost, and low synthesis temperature.

Many approaches have been reported for the mechanochemical synthesis of ZnO nanoparticles. Tsuzuki,[18] Moballegh,[20] and Weiqin[15] synthesised ZnO nanoparticles in a three-stage process consisting of mechanical milling, heat treatment, and washing, using $ZnCl_2$, Na_2CO_3 and NaCl as the reactants.
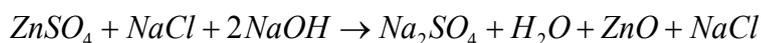
McCormick and Tzuzuki prepared ZnO nanoparticles from $ZnCO_3.2Zn(OH)_2$ and NaCl precursors through a mechanochemical method.[21] Lu, Ng and Yang synthesised ZnO nanoparticles from $ZnSO_4$, NaOH and NaCl in a one-step mechanochemical technique that eliminated the need for post-annealing.[22]

From a survey of literature, it can be observed that few attempts have been made to obtain ZnO nanoparticles using one-step mechanochemical methods. The major motive behind developing such a one-step mechanochemical method is the minimisation of the agglomeration of ZnO nanoparticles that plague materials synthesised by current techniques and to minimise the long reaction times required in conventional mechanochemical techniques. In this study, $ZnSO_4$, NaOH, and NaCl were utilised for the synthesis of ZnO nanoparticles. The effects of changing parameters such as the milling time, the order of synthesis stages, heat treatment on the particle size and optical properties have been investigated. The most important advantage of this approach, in comparison with other important studies, is the single-step nature of the mechanochemical synthesis and the utilisation of heat treatment only in the presence of a dilute phase, both of which serve to improve the photocatalytic activity of the zinc oxide nanostructure.

2.   EXPERIMENTAL

The precursors for the synthesis of ZnO nanoparticles were anhydrous $ZnSO_4$ (Aldrich, 99.5%) as a zinc source, 2 g of NaOH (Aldrich, 99.5%) as a reactant, and 10 g of NaCl (Aldrich, 99.8%) as a diluent.

The following reaction took place during the mechanochemical synthesis:

$$ZnSO_4 + NaCl + 2NaOH \rightarrow Na_2SO_4 + H_2O + ZnO + NaCl$$

The reaction was carried out in a planetary ball mill (ratchpm400) with a milling rate of 300 rpm and a ball-to-powder weight ratio (BPR) of 15:1. The molar ratio of NaCl to $ZnSO_4$ was fixed to 7.5:1.[22]

Zinc sulfate and NaCl were milled for 10 minutes. After the first milling process, a mixture of NaOH:$ZnSO_4$ with a molar ratio of 2:1 was added and the second milling process was carried out for different lengths of time. Table 1 lists the preparation parameters of various samples.

Table 1: Different mechanochemical synthesis conditions.

Sample	First milling time (min)	Second milling time (min)	Synthesis step arrangement
S1	10	20	Milled and washed
S2	10	30	Milled and washed
S3	10	20	Milled, heated and washed
S4	10	20	Milled, washed and heated

The NaCl and Na_2SO_4 were removed by washing with doubly deionised (DDI) water. The samples were dried in vacuum oven at 70°C for four hours. Heat treatment was carried out at 400°C for two hours with a $20°C.min^{-1}$ heating rate.

X-ray diffraction (XRD, Siemens D500, Cu Kα radiation) was used for phase identification and crystallite size determination. The crystallite sizes of the powders were estimated using the Scherrer equation and the full-width at half-maximum breadth of the relevant diffraction peaks. Scanning electron microscopy (SEM, Hitachi S-410 vacc 25kv microscope) and transmission electron microscopy (TEM, Phillips CM-200) analyses were carried out to evaluate the morphologies of the prepared nanoparticles. The optical properties of ZnO nanoparticles were studied using UV-Vis spectroscopy (PerkinElmer Spectrometer, LambdaIs USA) and photoluminescence (PL) analysis (Perkin Elmer, LS-5) with excitation wavelength of 320 nm.

Methyl orange (MO) (Merck) was applied as a model dye to evaluate the photocatalytic properties of the ZnO samples (catalysts). In a typical experiment, 12.5 mg of ZnO nanoparticles were dispersed in 50 ml of a 4 ppm MO aqueous solution. The photocatalytic experiments were performed at room temperature under a UV light placed horizontally above the liquid surface. Prior to irradiation, the solutions were placed in the dark for 24 hours to establish equilibrium in terms of the physical adsorption of the dye molecules. Every 20 minutes, 2 ml of the solution were withdrawn. Before UV-Vis analysis, the aqueous samples were centrifuged to remove any suspended solid catalyst particles. The rate of MO degradation by ZnO nanoparticles was calculated by the maximum absorbance of MO in the UV-vis spectrum, which occurs at 460 nm. The percentage of MO degradation was calculated using the following equation:

$$Ln(\frac{C}{C_0}) = -kt \tag{1}$$

Here, C is the dye concentration after irradiation, C_0 is the initial dye concentration, t is the irradiation time, and k is the photocatalytic activity.

3.   RESULTS AND DISCUSSION

Figure 1 shows the XRD patterns of synthesised ZnO nanocrystallites, revealing a single-phase hexagonal wurtzite pattern. As calculated by the Scherrer equation, the crystallite sizes of the S1 and S2 samples were 10.9 and 8.8 nm, respectively. These results indicated that an increase in milling time from 30 (S1 sample) to 40 minutes (S2 sample) led to increased collisions between particles and a decrease in particle size. The crystallite sizes of S3 and S4 samples were 18.4 and 21.3 nm, respectively, higher than S1 and S2 due to the crystallite growth induced by heat treatment. The difference between the S3 and S4 samples was the ordering of synthetic stages. While the synthetic stages of S3 sample were milling, then heating, followed by washing, the synthetic stages of the S4 sample placed milling first, followed by washing and, finally, heating.

NaCl was utilised as a diluent phase, prohibiting the agglomeration of particles during milling and heat treatment. The S3 sample was heated immediately after the milling process; therefore, NaCl and Na_2SO_4 were both present in the heat treatment stage. The S4 sample was instead washed after the milling process to remove the diluent phase, resulting in heat treatment without the presence of NaCl. The particles of the S4 sample were sintered during the heat treatment, resulting in crystallite sizes greater than found in S3.
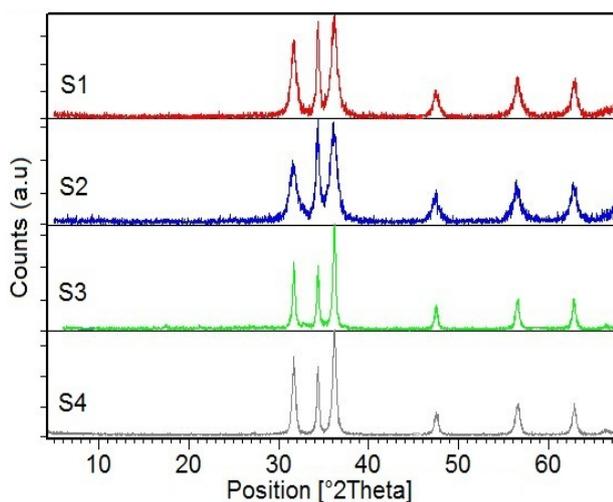

Figure 1: XRD patterns of the samples.

Figure 2 and Figure 3 depict the SEM and TEM images of the samples. The SEM images indicate that the particles of the S3 sample had not undergone significant growth owing to the presence of the NaCl diluent in the heat treatment stage. As illustrated in Figure 2, the only difference between the S1 and S3 samples was the slight agglomeration of particles in S3 sample after heat treatment. The TEM image of S1 shows irregular spheres and nanorods with sizes of ~50 nm. The TEM image of S4 shows particles sizes of approximately 80 nm.
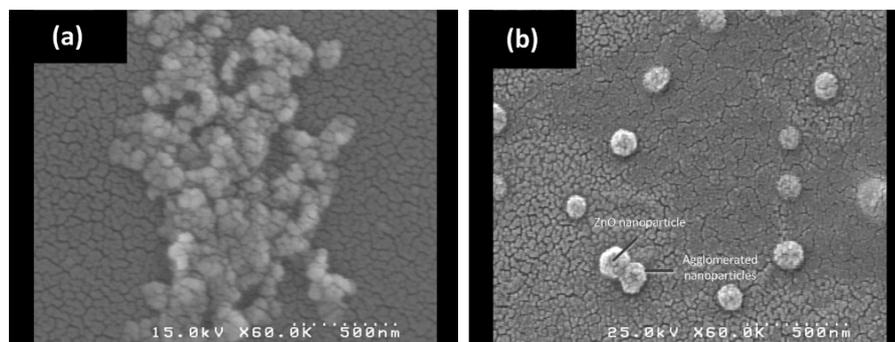

Figure 2:   SEM images of the samples (a) S1 (30 minutes milled and washed), (b) S3 (agglomerated nanoparticles during heat treatment).
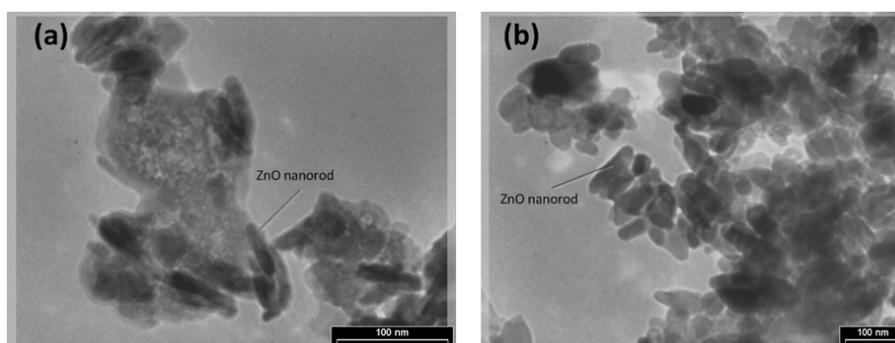

Figure 3: TEM images of the samples (a) S1 (particle size ~50 nm), (b) S4 (particle size ~80 nm).

ZnO nanoparticles were found to be transparent in the visible region of electromagnetic spectrum; however, they absorbed light in the UV range. The optical absorption spectra of samples are shown in the inset of Figure 4. Figure 4 shows the Tauc plots for different samples, which were applied to determine the optical band gap (E_g) of the ZnO nanoparticles, based on the following equation:

$$(\alpha h\nu) = A(h\nu - E_g)^n \tag{2}$$

For a semiconductor with a direct band gap, *n* is equal to 0.5. An indirect band gap semiconductor will show an *n* value equal to 2. In the equation above, ν is the photon frequency, *h* is the Planck's coefficient, α is the absorption coefficient, A is a constant, and E_g denotes the optical band gap. According to Figure 4, the optical band gaps of the samples were in the range of 3–3.21 eV. These values were smaller than band gap of bulk ZnO (3.37 eV) due to defects produced during the mechanochemical processes.[23] The optical band gap of the S2 sample was larger than found for S1, owing to the higher milling energy and smaller particle size. The optical band gap of S3 was smaller than S4 due to the greater defect population in the microstructure of the S3 sample.
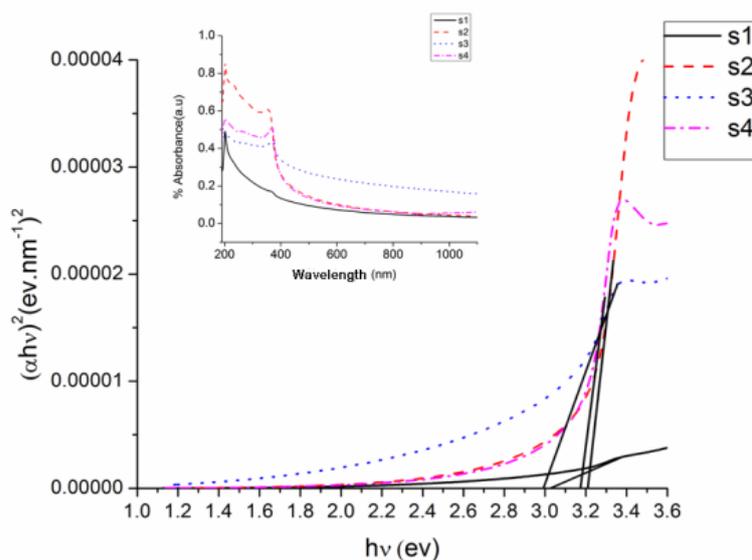

Figure 4: Tauc plots for different samples used calculate the band gap. The inset gives relevant UV-Vis absorption spectra.

Figure 5 presents the PL spectra of the samples, showing two peaks at 390 and 630 nm. The peak at 390 nm is in the UV range and is related to near-band-edge excitonic emission. The peak at 630 nm is related to the red emission, which is attributed to oxygen vacancies.[24] The red emission intensity of the S3 sample is greater than found for the other samples, indicating a higher concentration of defects in this sample.

Molten salts such as NaCl have a tendency to react with oxygen during heat treatment. Thus, in the heat treatment stage of the S3 sample, the NaCl present in the sample reacts with the oxygen within the ZnO nanostructure. This causes an increase in the number of oxygen vacancies, in agreement with

previous studies.[25] The red emission of the S2 sample can be attributed to the high surface oxygen vacancy concentration of this sample, as the average crystallite size in this sample was the smallest of those studied.[26] It is known that the high surface area to volume ratios in smaller nanoparticles favour higher levels of surface oxygen vacancies.
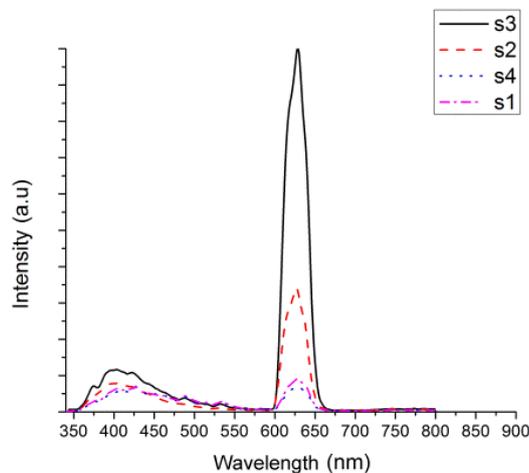

Figure 5: The PL spectra of the different samples collected at room temperature (the UV region at 390 nm and visible region at 630 nm).

Methyl orange (MO) can be photocatalytically degraded in the presence of ZnO nanoparticles under UV irradiation. Photo-generated holes and electrons drift to the surface of ZnO nanoparticles and react with adsorbed species, leading to the formation of superoxide radical anions, hydrogen peroxide and hydroxyl radicals, which degrade the dye molecule. The hydroxyl radical is highly reactive and is capable of oxidising many organic compounds. The photocatalytic activity of ZnO nanoparticles is schematically shown in Figure 6.
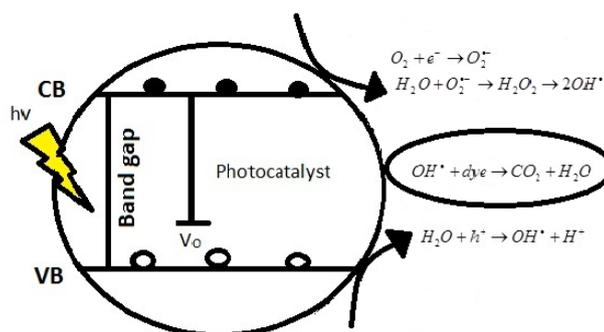

Figure 6: Photocatalytic activity of ZnO nanoparticles in MO degradation.

Figure 7 presents the photocatalytic activity of samples. The activities of the S3 and S2 samples were higher than found for the other samples, likely as a result of their higher concentrations of oxygen vacancies. In addition, the relatively high photocatalytic capacity of the S2 sample may also result from the smaller particle size within this sample. Smaller particle sizes serve to increase the specific surface area, thereby increasing the number of active surface sites where photogenerated charge carriers react with absorbed molecules in the formation of hydroxyl and superoxide radicals.[27]
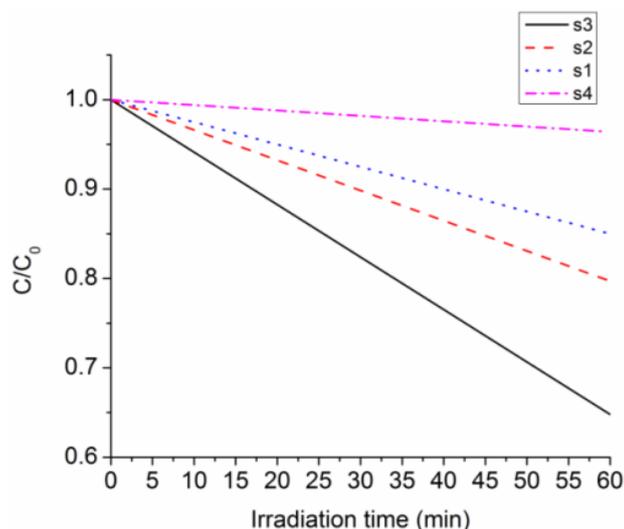

Figure 7:   The photocatalytic activities of S1 (30 minutes milled and washed), S2 (40 minutes milled and washed), S3 (30 minutes milled, heated and washed), and S4 (30 minutes milled, washed and heated).

In general, oxygen vacancies can act as electron-traps, allowing free holes to diffuse to the semiconductor surface and participate in the oxidation of organic molecules. Moreover, the decrease in electron density within the semiconductor leads to an increase in the hydroxyl group acidity, which in turn improves the photocatalytic activity.[28] Accordingly, higher concentrations of oxygen vacancies can significantly improve the photocatalytic activities of photocatalysts. In our case, it can be assumed that the surface oxygen vacancies improved the photocatalytic process through the successful separation of electron–hole pairs.

4.   CONCLUSION

The results of the current work showed that ZnO nanoparticles can be synthesised in a one-step method using $ZnSO_4$ and NaOH as reactants and NaCl as a diluent. Heat treatment in the presence of a diluent was applied to improve the photocatalytic activity of the resultant materials. The measured particle size in the samples was approximately 50 nm, with E_g values in the range of 3–3.21 eV, which are lower than bulk ZnO as a result of defects in the nanostructure. It was also found that the high surface areas (small crystallite size) and defect concentrations in the samples resulted in superior photocatalytic activities.

5.   ACKNOWLEDGEMENT

6.   REFERENCES

1.   Fu, Y. S. et al. (2010). ZnO hierarchical nanostructures and application on high-efficiency dye-sensitized solar cells. *Mater. Sci. Eng.*, 166(3), 196–202.
2.   Hong, R. Y. et al. (2009). Synthesis, surface modification and photocatalytic property of ZnO nanoparticles. *Powder Technol.*, 189(3), 426–432.
3.   Hsu, C. -L. et al. (2013). Fabrication of gas sensor based on p-type ZnO nanoparticles and n-type ZnO nanowires. *Sens. Actuators B*, 182, 190–196.
4.   Pauporté, T. & Lincot, D. (2000). Electrodeposition of semiconductors for optoelectronic devices: Results on zinc oxide. *Electrochimica Acta.*, 45(20), 3345–3353.
5.   Abrarov, S. M. et al. (2005). Effect of photonic band-gap on photoluminescence of ZnO deposited inside the green synthetic opal. *Opt. Commun.*, 250(1–3), 111–119.
6.   Rusdi, R. et al. (2011). Preparation and band gap energies of ZnO nanotubes, nanorods and spherical nanostructures. *Powder Technol.*, 210(1), 18–22.
7.   Lanje, A. S. et al. (2013). Low temperature dielectric studies of zinc oxide (ZnO) nanoparticles prepared by precipitation method. *Adv. Powder Technol.*, 24(1), 331–335.
8.   Kumar, S. S. et al. (2013). Synthesis, characterization and optical properties of zinc oxide nanoparticles. *Int. Nano. Lett.*, 3(30): 1–6.

9.   Lee, S. D. et al. (2012). Synthesis and photocatalytic property of ZnO nanoparticles prepared by spray-pyrolysis method. *Phys. Procedia*, 32, 320–326.

10.   Kumar, S. & Sahare, P. D. (2012). Observation of band gap and surface defects of ZnO nanoparticles synthesized via hydrothermal route at different reaction temperature. *Opt. Commun.*, 285(24), 5210–5216.

11.   Ba-Abbad, M. M. et al. (2013). The effect of process parameters on the size of ZnO nanoparticles synthesized via the sol–gel technique. *J. Alloys Compd.*, 550, 63–70.

12.   Li, Q. et al. (2013). Photoluminescence and wetting behaviour of ZnO nanoparticles/nanorods array synthesized by thermal evaporation. *J. Alloys Compd.*, 560, 156–160.

13.   Sendi, R. K. & Mahmud, S. (2012). Quantum size effect on ZnO nanoparticle-based discs synthesized by mechanical milling. *Appl. Surf. Sci.*, 258(20), 8026–8031.

14.   Aghababazadeh, R. et al. (2006). ZnO nanoparticles synthesised by mechanochemical processing. *J. Phys.*, 26, 312.

15.   Ao, W. et al. (2006). Mechanochemical synthesis of zinc oxide nanocrystalline. *Powder Technol.*, 168(3), 148–151.

16.   Shen, L. et al. (2006). Direct synthesis of ZnO nanoparticles by a solution-free mechanochemical reaction. *Nanotechnol.*, 17(20), 5117.

17.   Shen, L. et al. (2003). Salt-assisted solid-state chemical reaction. Synthesis of ZnO nanocrystals. *Chem. Lett.*, 32(9), 826–827.

18.   Tsuzuki, T. & McCormick, P. G. (2004). Mechanochemical synthesis of nanoparticles. *J. Mater. Sci.*, 39(16–17), 5143–5146.

19.   Yang, H. et al. (2004). Formation of zinc oxide nanoparticles by mechanochemical reaction. *Mater. Sci. Technol.*, 20(11), 1493–1495.

20.   Moballegh, A. et al. (2007). ZnO nanoparticles obtained by mechanochemical technique and the optical properties. *Sur. Sci.*, 601(13), 2850–2854.

21.   McCormick, P. G. & Tzuzuki, T. (2003). *Process for the production of ultrafine powders of metal oxides*. US Patent 6,503,475, Google Patents.

22.   Lu, J., Ng, K. M. & Yang, S. (2008). Efficient, one-step mechanochemical process for the synthesis of ZnO nanoparticles. *Ind. Eng. Chem. Res.,* 47(4), 1095–1101.

23.   Zandi, S. et al. (2011). Microstructure and optical properties of ZnO nanoparticles prepared by a simple method. *Physica B: Condensed Matter*, 406(17), 3215–3218.

24.   Singh, A., Viswanath, V. & Janu, V. (2009). Synthesis, effect of capping agents, structural, optical and photoluminescence properties of ZnO nanoparticles. *J. Lumin.*, 129(8), 874–878.

25.   Li, Y. X. et al. (2005). Synthesis of CeO$_2$ nanoparticles by mechanochemical processing and the inhibiting action of NaCl on particle agglomeration. *Mater. Lett.*, 59(1), 48–52.
26.   Huang, M. H. et al. (2001). Catalytic growth of zinc oxide nanowires by vapor transport. *Adv. Mater.*, 13(2), 113–116.
27.   Dodd, A. et al. (2006). Effect of particle size on the photocatalytic activity of nanoparticulate zinc oxide. *J. Nanopart. Res.*, 8(1), 43–51.
28.   Wang, H. & Xie, C. (2008). The effects of oxygen partial pressure on the microstructures and photocatalytic property of ZnO nanoparticles. *Physica E Low Dimens. Syst. Nanostruct.*, 40(8), 2724–2729.